Check for updates

Lacticaseibacillus casei HY2782 improves the intestinal barrier and tract environment and ultimately prolongs the lifespan of *Caenorhabditis elegans*†

Won-Young Bae,‡[a] Uyen Tran Tu Nguyen,‡[a,b] Tram Anh Ngoc Le,[a] Son Hung Tran,[a,b] Sohyun Lee,[a,b] Sung-Chul Hong,[a,c] Kwang Hyun Cha,[a,b] Il-Dong Choi[d] and Kyungsu Kang (ID) *[a,b]

Caenorhabditis elegans is widely used as a model for investigating longevity owing to its short life cycle and the presence of human orthologs. This study aimed to ultimately prolong the lifespan of *C. elegans* by evaluating the gastrointestinal tract conditions and intestinal permeability of *C. elegans* fed *Lacticaseibacillus casei* HY2782 alone or fermented fecal products. The anti-inflammatory effects of *L. casei* HY2782 were determined based on interleukin 8 (IL-8) levels and intestinal permeability in human intestinal epithelial cells. In the *C. elegans* model, intestinal permeability was assessed in the N2 wild-type as well as *skn-1*, *pmk-1*, *daf-16*, and *aak-2* mutant worms. During simulated colonic fecal fermentation, changes in short chain fatty acid and microbial composition were investigated. *L. casei* HY2782 reduced IL-8 production and intestinal permeability from 1646.8 to 1009.1 pg mL^{-1} and 265.5 to 115.1%, respectively ($p < 0.01$). Additionally, *L. casei* HY2872 attenuated intestinal leakage in *C. elegans* and prolonged its lifespan *via* the DAF-16/FOXO and SKN-1/NRF2 pathways and *gst-4* gene expression. Moreover, *L. casei* HY2782 inhibited intestinal leakage in aged worms. During fermentation, *L. casei* HY2782 produced butyrate under both normal and high-protein conditions. Additionally, *L. casei* HY2782 contributed to butyrate production by genera, such as *Faecalibacterium* and *Lachnospira* ($p < 0.01$), while inhibiting *Fusobacterium* ($p < 0.05$). *L. casei* HY2782 also prolonged lifespan of intestinally damaged worms ($p < 0.001$). Furthermore, *C. elegans* fed *L. casei* HY2782-fermented fecal products lived significantly longer than those fed the vehicle control ($p < 0.001$). Overall, *L. casei* HY2782 restored the intestinal tract by mitigating inflammation and microbial metabolic dysbiosis, ultimately extending the lifespan of *C. elegans*.

1. Introduction

The popularity of high-protein diets has grown steadily owing to their effectiveness in promoting rapid weight loss.[1] Not only individuals with obesity, but also weight-class athletes, such as physique and bodybuilding athletes, consume high-protein

[a]*Center for Natural Product Systems Biology, Gangneung Institute of Natural Products, Korea Institute of Science and Technology (KIST), Gangneung, Gangwon-do, 25451, South Korea. E-mail: kskang@kist.re.kr*

[b]*Natural Product Applied Science, KIST School, University of Science and Technology (UST), Gangneung, Gangwon-do, 25451, South Korea*

[c]*Department of Food Science and Biotechnology, Kunsan National University, Gunsan, Jeollabuk-do, 54150, South Korea*

[d]*R&BD Department, hy Co., Ltd, Yongin, Gyeonggi-do, 17086, South Korea*

†Electronic supplementary information (ESI) available. See DOI: https://doi.org/10.1039/d5fo01239b

‡These authors contributed equally to this work.

diets to reduce their body-fat ratio.[2] Combined with low-carbohydrate diets, high-protein diets improve glycated hemoglobin levels in patients with type 2 diabetes.[3] However, chronic high-protein diets result in intestinal permeability, systemic inflammation, and gut microbiome loss, including *Bacteroides* and *Akkermansia*.[1]

Dr Élie Metchnikoff proposed Metchnikoff's hypothesis, which postulated that probiotics contributed to the longevity of Bulgarian peasants. Metchnikoff's hypothesis was based on yogurt containing lactic acid bacteria (LAB) and contributed to shaping the role of probiotics.[4] Probiotics are live microorganisms that improve host health when consumed in adequate amounts.[5,6] The beneficial effects of probiotics, including regulation of the microbiome and immune system, result from a healthy gut.[4,5] However, aging disrupts the immune and digestive systems and the gut microbiome balance, leading to intestinal inflammation.[5] *Caenorhabditis elegans* (*C. elegans*) is

a small nematode that has a short life cycle.[4,5,7–13] An aged *C. elegans* shares similarities with the aged intestine in mammals, including poor permeability, small and fewer microvilli, and decreased digestive ability.[9] Therefore, *C. elegans* models have been used to elucidate the correlation between aging and the consumption of functional foods and probiotics.[5,6,9,14]

Lacticaseibacillus casei (*L. casei*) is a facultative heterofermentative LAB, typically present in fermented dairy products, vegetables, and the gastrointestinal (GI) tracts of humans and other animals.[15] Moreover, *L. casei* DN-114001, which is used to ferment yogurt, alleviates atopic dermatitis in children.[16] Similarly, *L. casei* HY2782, a probiotic strain isolated from human feces, alleviates depression[17] and attenuates cellular and physiological toxicity induced by particulate matter.[18] However, the health effects of *L. casei* HY2782, particularly related to the regulation of aging and longevity, are not fully understood. Moreover, many studies have focused on short-chain fatty acid (SCFA) production by probiotics; however, a comparison of SCFA production under a normal and high-protein diet under simulated colonic conditions has not yet been reported.

Therefore, this study aimed to evaluate the gut conditions and lifespan of *C. elegans* fed *L. casei* HY2782 bacteria alone or *L. casei* HY2782-fermented fecal fermentation products. Moreover, the study compared SCFA production under a normal and high-protein diet under simulated colonic conditions. Ultimately, Metchnikoff's hypothesis was evaluated, thereby revealing the correlation between gut environment and longevity.

2. Materials and methods

2.1 Reagents, microorganisms, and cell culture

Recombinant human interleukin (IL)-1β was purchased from PeproTech (Rocky Hill, NJ, USA). Fluorescein isothiocyanate–dextran (FITC-dextran, average molecular weight = 4 kDa), 3,3′-diindolylmethane (DIM), 2-methylpentanoic acid, and volatile-free acid mix were obtained from Sigma-Aldrich (St. Louis, MO, USA). Brilliant Blue FCF dye was purchased from Tokyo Chemical Industry (Tokyo, Japan).

The *L. casei* HY2782 was provided by hy Co. Ltd (Yongin, Korea) and was cultured in de Man-Rogosa-Sharpe medium (BD Biosciences, Franklin Lakes, NJ, USA) at 37 °C for 24 h. *Pseudomonas aeruginosa* ATCC 15692 (PAO1) (*P. aeruginosa* PAO1) was obtained from the American Type Culture Collection (Manassas, VA, USA), and *Escherichia coli* (*E. coli*) OP50 was obtained from *Caenorhabditis* Genetics Center (Minneapolis, MN, USA). *P. aeruginosa* PAO1 and *E. coli* OP50 were cultured in Luria Bertani broth at 37 °C for 15 h at an agitation speed of 150 rpm.

Human intestinal epithelial cells (HT-29 and Caco-2) were purchased from the Korean Cell Line Bank (Seoul, Korea). The cells were maintained in Dulbecco's modified Eagle's medium (Cytiva, Marlborough, MA, USA) supplemented with 10% fetal bovine serum and 1% penicillin–streptomycin solution at 37 °C in a humidified atmosphere containing 5% CO_2. During incubation, the medium was replaced every 2–3 d, and the cells were grown until they reached 80% confluence. For differentiation, Caco-2 cells (4×10^5 cells) were seeded in a 60 mm culture dish, and the medium that contained 1% (v/v) nonessential amino acid solution was changed every two days as described previously.[19,20]

2.2 Evaluation of cell viability and IL-8 production

HT-29 cells were seeded in 96-well microplates (1×10^4 cells per well) and incubated for 24 h. After incubation, the HT-29 cells were treated with DIM (10 μM) or 5×10^7 colony-forming unit (CFU) mL^{-1} of *L. casei* HY2782 for 24 h. An inflammatory reaction was induced by adding IL-1β (10 ng mL^{-1}) to DIM- or *L. casei* HY2782-treated cells for 5 h. DIM was used as a positive control because it exerts anti-inflammatory activity in intestinal epithelial cells.[19] Following reaction completion, the supernatants were harvested and centrifuged at 2000*g* for 20 min at 4 °C. IL-8 production in the supernatant was analyzed using ELISA MAX™ Deluxe Set Human IL-8 (BioLegend, San Diego, CA, USA) according to the manufacturer's guidelines. The viability of DIM- or *L. casei*-treated cells was measured using an EZ-Cytox kit (DoGenBio, Seoul, Korea). The absorbance of water-soluble tetrazolium salts was measured at 450 nm using a microplate reader (Synergy HTX Multi-Mode Reader; BioTek, Winooski, VT, USA).[19,20]

2.3 Assessment of cellular permeability in human intestinal epithelial cells

Intestinal permeability was investigated by measuring the transepithelial electrical resistance (TEER) and FITC-dextran efflux in Caco-2 cells.[18–20] Briefly, 3×10^5 Caco-2 cells per well were seeded on the apical side of a 12-well Transwell® microplate. The cells were cultured for 12–15 days to allow differentiation into a polarized monolayer. Following polarization, the cells were treated with IL-1β (50 ng mL^{-1}) and DIM (10 μM) or 5×10^7 CFU mL^{-1} of *L. casei* HY2782 for 72 h. DIM was used as a positive control as it recovered the intestinal barrier function in cultured Caco-2 cell monolayers.[19] The change in TEER values was measured using a Millicell® ERS-2 Electrical Resistance System (MilliporeSigma, Burlington, MA, USA). After TEER measurements, the medium on the apical side was removed and replaced with fresh medium containing 1 mg mL^{-1} FITC-dextran. FITC-dextran efflux was then performed for 2 h, and the fluorescence intensity of the basolateral side was evaluated using a microplate reader (Infinite® M1000; Tecan, Männedorf, Switzerland) at 485 nm excitation and 535 nm emission wavelengths.

2.4 *C. elegans* maintenance

The *C. elegans* wild-type N2 Bristol variety was used with the following mutant strains: EU31, *skn-1*(zu135) IV/nT1 [unc-? (n754) let-?] (IV;V); KU25, *pmk-1*(km25) IV; CF1038, *daf-16* (mu86) I; RB754, *aak-2*(ok524) X; and CL2166, *dvIs19* [(*pAF15*) *gst-4p::GFP::NLS*] *III*. All strains were maintained on nematode

growth media (NGM) at 20 °C, seeded with *E. coli* OP50 as a food source. Synchronized L4 worms were examined for intestinal permeability and lifespan.[10,19,20]

2.5 Intestinal permeability in *L. casei* HY2782-treated *C. elegans*

The *P. aeruginosa* PAO1 cell-free supernatant (CFS) was prepared using a 0.45 µm membrane filter. Larvae at the synchronized L4 stage were transferred onto NGM agar and incubated with 795 µL of *E. coli* OP50 or *L. casei* HY2782 ($\sim 1 \times 10^8$ CFU mL^{-1}) for 48 h. During incubation, *C. elegans* was treated with 5 µL of CFS to induce intestinal permeability dysfunction. After incubation, all worms were washed with S-buffer and further incubated with FITC-dextran (20 µg mL^{-1}) and *E. coli* OP50 for 15 h. The FITC-dextran-treated worms were washed with S-buffer and fixed with 4% formaldehyde. All fixed worms were mounted using mounting media in a 96-well microplate and observed using a high content analysis system (Operetta® CLS™; PerkinElmer, Waltham, MA, USA) with an enhanced green fluorescent protein (EGFP) filter.[10,19,20]

2.6 Lifespan measurement of intestinal-damaged *C. elegans*

Synchronized worms (L4 stage) were transferred onto NGM agar (60 mm) coated with 20 µL of *P. aeruginosa* CFS mixed in 380 µL of *E. coli* OP50 or *L. casei* HY2782 culture.[21] After incubation, the plates were observed under a stereomicroscope (SMZ800N; Nikon, Tokyo, Japan). Worms that did not respond to gentle poking with a platinum wire were considered dead.[7,9,19]

2.7 Detection of Smurf phenotype in aged worms

The physiological condition of aged worms was observed using the Smurf assay with slight modifications.[22] Briefly, age-synchronized L4-stage worms were transferred onto NGM agar (60 mm) supplemented with *E. coli* OP50 or *L. casei* HY2782. On day 10 of adulthood, worms were collected and washed with S-buffer. The washed worms were incubated in Brilliant Blue FCF dye 5% (w/v) for 3 h at 20 °C except for the vehicle control (non-dyed worms). Worms on day 4 of adulthood that were fed *E. coli* OP50 were used as non-Smurf worms. Representative images were taken with a stereomicroscope (SMZ800N; Nikon). Worms exhibiting blue dye in the germline only were not classified as Smurf worms unless the dye also leaked into the body cavity.

2.8 Glutathione *S*-transferase 4 gene (*gst-4*) expression in transgenic worms

The CL2166 worm strain, which contains the *gst-4p::GFP* reporter construct, was synchronized at the L4 stage. After synchronization, the worms were transferred onto NGM agar coated with *E. coli* OP50 alone, *L. casei* HY2782 alone, *E. coli* OP50 mixed with *P. aeruginosa* CFS, or *L. casei* HY2782 mixed with *P. aeruginosa* CFS. The GFP expression was evaluated using a High Content Analysis System with an EGFP filter at 24, 48, and 72 h.[11]

2.9 Simulated colonic fecal fermentation with *L. casei* HY2782

2.9.1 Preparation of human fecal samples. Collection of human fecal samples was approved by the Institutional Review Board of the Korea Institute of Science and Technology, Seoul, Korea (Approval number: 2018-009). All donors provided written informed consent prior to enrollment, and all procedures were performed in accordance with the guidelines of the Declaration of Helsinki. The participants had no underlying medical conditions and had not taken any antibiotics or probiotics before the study for at least three months.[23,24] All specimens were harvested using a stool sample collection kit (Fisherbrand Commode Specimen Collection System; Thermo Fisher Scientific, Waltham, MA, USA) and were immediately transferred to an anaerobic chamber for temporary maintenance before injection into a bioreactor.[24]

2.9.2 Simulation of colonic fecal fermentation. To simulate colonic fecal fermentation, artificial normal colonic conditions were used, as described in a previous study.[24] The specific medium compositions are shown in Table S1.† Casein was added to simulate a high-protein diet colon. To develop artificial colon conditions, 12.5% (v/v) fecal slurry was injected into normal colon or high-protein diet medium. The development of artificial colon conditions was conducted in a bioreactor (FMT DS-M6-01; Fermentec, Cheongju, Korea) at 37 °C for one week under anaerobic conditions through continuous N$_2$ flushing (20 mL min^{-1}). The pH value of each bioreactor was automatically adjusted to pH 6.2 using 1 N sodium bicarbonate and 1 N sodium hydroxide. After one week, 5×10^7 CFU mL^{-1} of *L. casei* HY2782 was injected into each reactor daily and further fermented for 10 d. During *L. casei* HY2782 fermentation, the medium was harvested on days 1, 2, 4, and 10. All collected samples were stored at −80 °C until SCFA analysis and 16S rRNA metagenome amplicon sequencing.

2.9.3 SCFA analysis of media fermented under simulated colonic fecal fermentation. The SCFA content in the fermented media samples was analyzed using a gas chromatography system coupled with a flame ionization detector (GC-FID). SCFAs were extracted from the fermented media samples *via* acidification.[24,25] Briefly, 500 µL of the fermented media samples was treated with 50% sulfuric acid at 25 °C for 5 min. After acidification, the acidic solution was collected *via* centrifugation at 14 000*g* for 10 min. The supernatants were further extracted to obtain fatty acids by adding 500 µL of anhydrous ethyl ether and shaking for 30 s. Following centrifugation at 14 000*g* for 10 min, the fatty acids were collected in the upper ether layer, and 2-methylpentanoic acid (1%) was used as an internal standard.

The GC-FID system comprised a Bruker Varian 450-GC instrument (Bruker Corporation, Billerica, MA, USA). A Nukol™ Capillary GC Column (30 m × 0.25 mm, 0.25 µm film thickness; Supelco, Burlington, MA, USA), which is an acid-modified polyethylene glycol phase column, was employed. The injection port and flame ionization detector temperature were maintained at 225 °C. The sample injection volume was 2 µL in splitless mode. Nitrogen was applied as the carrier gas, and oven temperature was maintained at 170 °C. A 10 mM

volatile-free acid mix was used as a certified reference material for quantification.

2.9.4 16S rRNA metagenome amplicon sequencing. During fermentation, samples of both the vehicle control (fermented fecal sample without *L. casei* HY2782) and *L. casei* HY2782-injected groups were harvested to analyze microbiome changes. Genomic DNA was extracted from each sample using a QIAamp DNA Stool Mini Kit (QIAGEN, Hilden, Germany) with an additional bead-beating step to improve DNA recovery from Gram-positive bacteria.[23] The V3–V4 region (319F/806R) of the 16S rRNA gene amplicons was prepared, as described by Fadrosh *et al.*[26] PCR amplicons were purified using AMPure XT beads (Beckman Coulter, Brea, CA, USA) and quantified using Qubit dsDNA High Sensitivity Reagent (Invitrogen, Waltham, MA, USA). The 16S rRNA gene amplicons were used for library construction, and paired-end sequencing (2 × 300 bp) was performed on a MiSeq platform (Illumina, San Diego,

CA, USA). Raw-read sequences were demultiplexed, assembled, and quality filtered using QIIME 2 with default settings.[27] A Naïve Bayes classifier was trained using the 16S rRNA region (V3–V4), primer set, and read length (469 bp). Taxonomic classification was performed using Greengene-formatted databases. The operational taxonomic unit (OTU) was detected at a genetic distance of 0.03 (with 97% sequence similarity). The sequence data were deposited in the Sequence Read Archive under the accession number PRJNA1071338. Integrative microbiome data analysis was performed using MicrobiomeAnalyst (**https://www.microbiomeanalyst.ca/**).[28]

2.9.5 Lifespan comparison under simulated colon conditions. Synchronized worms (L4 stage) were transferred onto NGM agar containing the fermented media samples. During incubation, the plates were observed under a stereomicroscope (SMZ800N; Nikon). Worms that did not respond to gentle poking with a platinum wire were considered dead.[7,9,19]
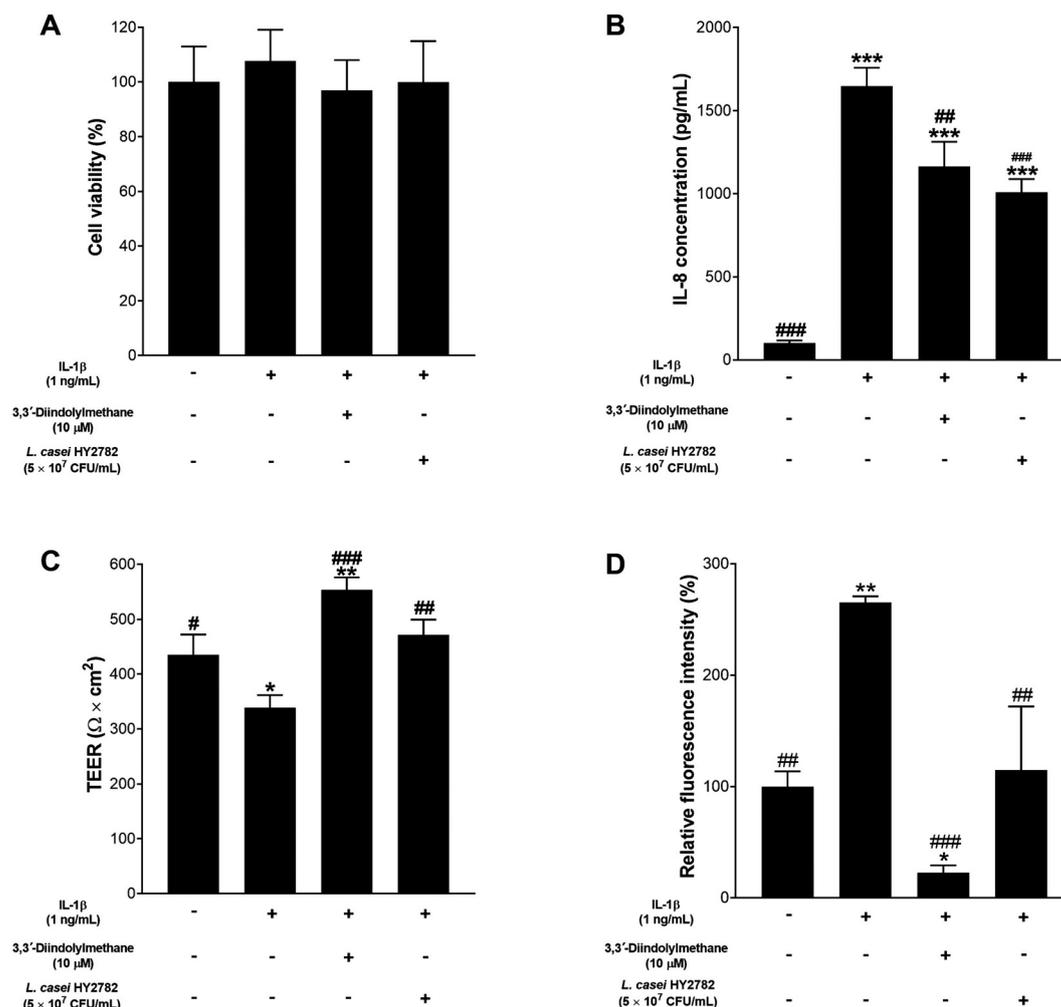

Fig. 1 Effect of *Lacticaseibacillus casei* HY2782 on interleukin (IL)-1β-induced inflammation in intestinal epithelial cells. (A) Relative cell viability of HT-29 cells. (B) Comparison of IL-8 production in HT-29 cells under inflammation. (C) Transepithelial electrical resistance (TEER) values of the differentiated Caco-2 cells. (D) Relative fluorescein isothiocyanate-dextran (FITC-dextran) permeabilities in the differentiated Caco-2 cells. Data are shown as mean ± standard deviations of three independent experiments. Mean values were analyzed using one-way analysis of variance (ANOVA), followed by Tukey's range test. Significant differences compared with the vehicle control (*$p < 0.05$, **$p < 0.01$, and ***$p < 0.001$) and IL-1β-treated group without 3,3'-diindolylmethane or *L. casei* HY2782 (#$p < 0.05$, ##$p < 0.01$, and ###$p < 0.001$) are shown.

2.10 Statistical analysis

Statistical analyses were performed using JMP version 13 (JMP Statistical Discovery, Cary, NC, USA). Mean values were analyzed using student's t-test and one-way ANOVA followed by Tukey's range, Duncan's multiple range, and Games-Howell at $p < 0.05$. To analyze the lifespan of $C.$ $elegans$, the two groups were compared using the log-rank test, with significance set at $p < 0.05$. To analyze Smurf phenotype in aged worms, the two groups were compared using a binomial test at $p < 0.05$.

3. Results

3.1 Anti-inflammatory effects of L. casei HY2782 in human intestinal epithelial cells

The IL-8 production and intestinal permeability of human intestinal cells treated with $L.$ $casei$ HY2782 are shown in Fig. 1. $L.$ $casei$ HY2782 did not exhibit cytotoxicity in HT-29 cells (Fig. 1A). Moreover, $L.$ $casei$ HY2782 significantly decreased IL-8 levels from 1646.8 to 1009.1 pg mL^{-1} ($p < 0.001$) in HT-29 cells under IL-1β-induced inflammation (Fig. 1B). Furthermore, IL-1β significantly decreased the TEER value from 478 to 329 Ω cm^2 ($p < 0.01$), whereas that in $L.$ $casei$ HY2782-treated cells slightly decreased from 478 to 439 Ω cm^2 (Fig. 1C). In addition, $L.$ $casei$ HY2782 significantly decreased FITC-dextran permeability from 265.5 to 115.1% ($p < 0.01$, Fig. 1D). Taken together, $L.$ $casei$ HY2782 exerted anti-inflammatory effects and improved intestinal barrier function in the cultured human intestinal cells.

3.2 Inhibition of intestinal permeability in C. elegans by L. casei HY2782

To evaluate the effect of $L.$ $casei$ HY2782 on the intestinal barrier function of $C.$ $elegans$, the intestinal FITC-dextran permeability was determined using fluorescence microscopy. As shown in Fig. 2, $P.$ $aeruginosa$ PAO1 CFS induced significant gut leakage and permeability of FITC-dextran in wild-type $C.$ $elegans$ ($p < 0.001$, Fig. 2). However, $L.$ $casei$ HY2782 significantly decreased FITC-dextran permeability in $C.$ $elegans$ administered $P.$ $aeruginosa$ CFS ($p < 0.05$) (Fig. 2B).

Mutant worms that were deficient in skn-1, pmk-1, daf-16, or aak-2 were used to identify the genes responsible for the beneficial effects of $L.$ $casei$ HY2782. In contrast to the wild-type, skn-1, daf-16, and aak-2 mutant worms did not show $L.$ $casei$ HY2782-induced recovery from gut leakage (Fig. 3, 5 and 6). However, the pmk-1 mutant (KU25) showed a significant decrease in fluorescence intensity from 175.1% to 54.6% ($p < 0.001$) (Fig. 4). These results indicate that skn-1, daf-16, and aak-2 are involved in the $L.$ $casei$ HY2782-facilitated recovery of intestinal permeability in $C.$ $elegans$.

3.3 Effect of L. casei HY2782 consumption on lifespan of C. elegans damaged by P. aeruginosa

To further verify whether the improvement in intestinal permeability by $L.$ $casei$ HY2782 was associated with lifespan extension, the effect of $L.$ $casei$ HY2782 consumption on lifespan extension was examined in $P.$ $aeruginosa$ CFS-treated $C.$ $elegans$. As shown in Table 1 and Fig. 7, the control group ($E.$ $coli$ OP50 with $P.$ $aeruginosa$ CFS) exhibited a shorter mean lifespan of 8.5 ± 0.3 days and a maximum lifespan of 21 days than those of $L.$ $casei$ HY2782 feeding group ($L.$ $casei$ HY2782 with $P.$ $aeruginosa$ CFS). Conversely, $L.$ $casei$ HY2782 extended the mean lifespan to 12.1 ± 0.4 days and maximum lifespan to 25 days ($p < 0.001$).

3.4 Effect of L. casei HY2782 consumption on intestinal permeability in aged C. elegans

To further investigate the improvement of intestinal permeability induced by $L.$ $casei$ HY2782 consumption, the incidence of Smurf phenotype was examined in $L.$ $casei$ HY2782-fed aged $C.$ $elegans$

Fig. 2 Effect of $Lacticaseibacillus$ $casei$ HY2782 on $Pseudomonas$ $aeruginosa$ PAO1 cell-free supernatant (CFS)-induced intestinal permeability dysfunction in $Caenorhabditis$ $elegans$. (A) Fluorescent microscopic observation of $C.$ $elegans$. (B) Quantification of fluorescence intensity in $C.$ $elegans$. The relative fluorescence intensities were measured by comparison with that of the CFS-treated group. Data are shown as mean ± standard deviations of three independent experiments. Mean values were analyzed using one-way analysis of variance (ANOVA), followed by Tukey's range test. Significant differences compared with the control ($Escherichia$ $coli$ OP50-fed group, ***$p < 0.001$) and CFS-fed group ($E.$ $coli$ OP50 mixed with CFS, #$p < 0.05$ and ###$p < 0.001$) are shown.
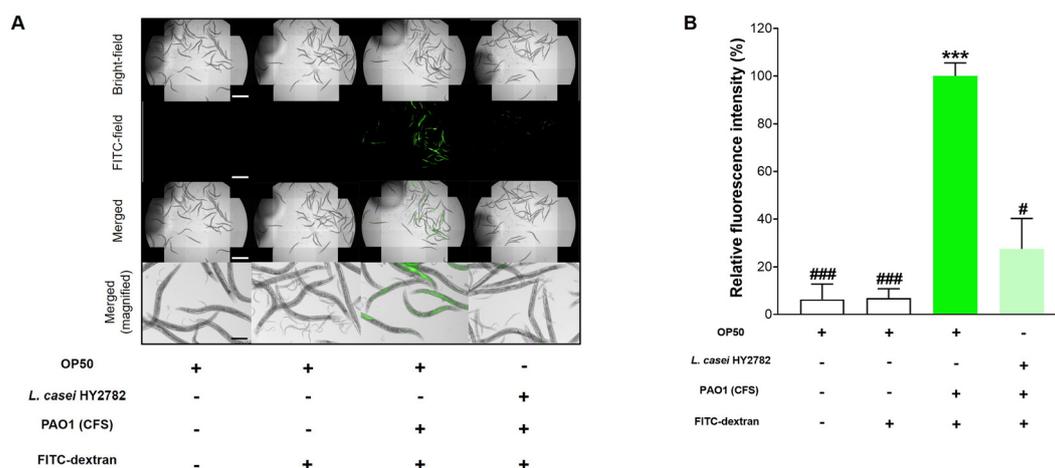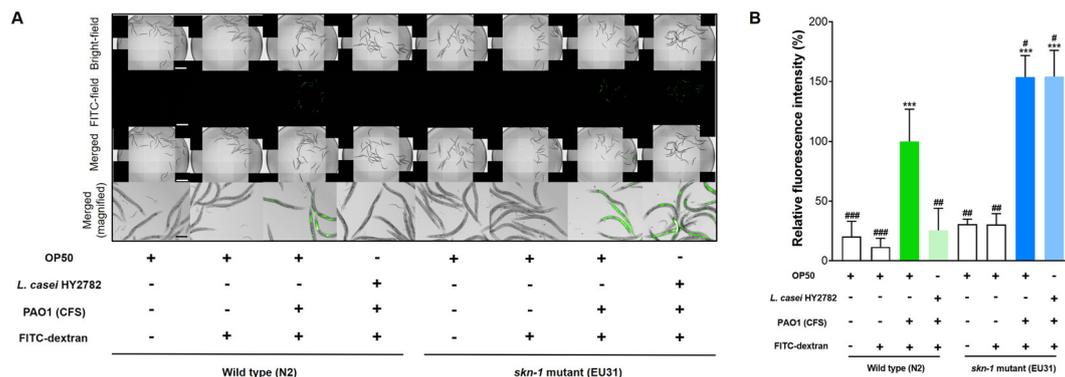
Fig. 3 Effect of *Lacticaseibacillus casei* HY2782 on *Pseudomonas aeruginosa* PAO1 cell-free supernatant (CFS)-induced intestinal permeability dysfunction in wild-type and *skn-1* mutant *Caenorhabditis elegans*. (A) Fluorescent microscopic observation of *C. elegans*. (B) Quantification of fluorescence intensity in *C. elegans*. The relative fluorescence intensities were measured by comparison with that of the CFS-treated group. Data are shown as mean ± standard deviations of three independent experiments. Mean values were analyzed using one-way analysis of variance (ANOVA), followed by Tukey's range test. Significant differences compared with the control (*Escherichia coli* OP50-fed group, ***$p < 0.001$) and CFS-fed group (*E. coli* OP50 mixed with CFS, #$p < 0.05$, ##$p < 0.01$, and ###$p < 0.001$) are shown.
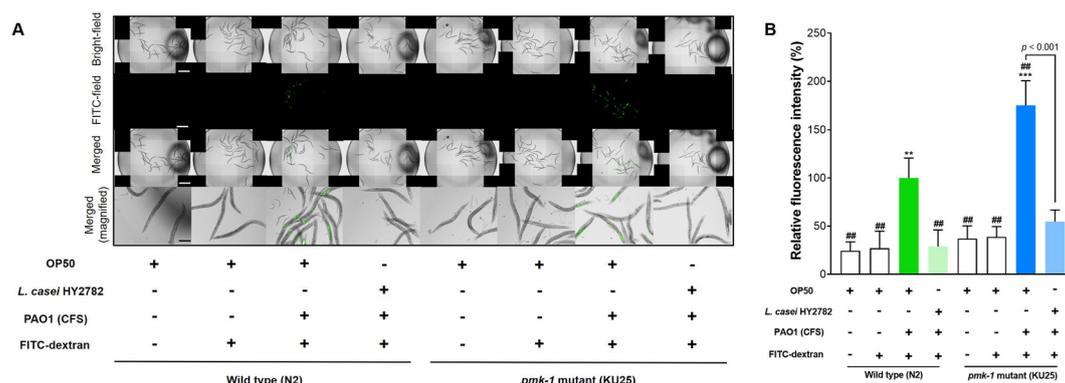

Fig. 4 Effect of *Lacticaseibacillus casei* HY2782 on *Pseudomonas aeruginosa* PAO1 cell-free supernatant (CFS)-induced intestinal permeability dysfunction in wild-type and *pmk-1* mutant *Caenorhabditis elegans*. (A) Fluorescent microscopic observation of *C. elegans*. (B) Quantification of fluorescence intensity in *C. elegans*. The relative fluorescence intensities were measured by comparison with the CFS-treated group. Data are shown as means ± standard deviations of three independent experiments. Mean values were analyzed using one-way analysis of variance (ANOVA), followed by Tukey's range test. Significant differences compared with the control (*Escherichia coli* OP50-fed group, **$p < 0.01$ and ***$p < 0.001$) and CFS-fed group (*E. coli* OP50 mixed with CFS, ##$p < 0.01$) are shown.
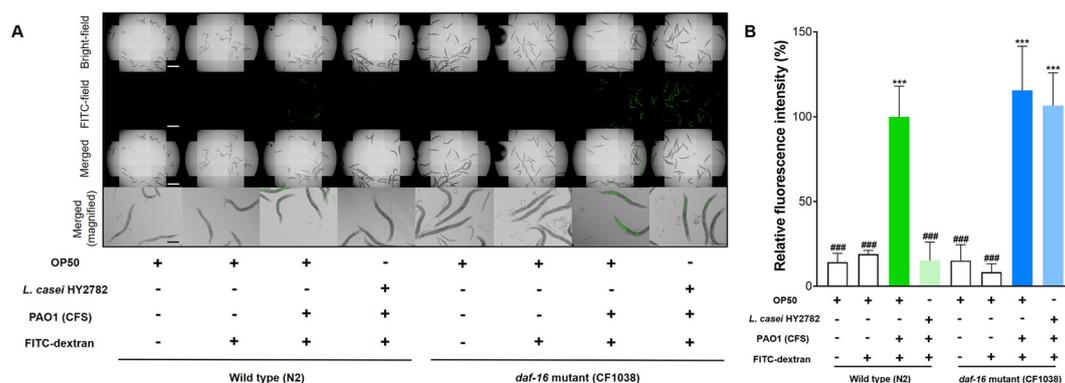

Fig. 5 Effect of *Lacticaseibacillus casei* HY2782 on *Pseudomonas aeruginosa* PAO1 cell-free supernatant (CFS)-induced intestinal permeability dysfunction in wild-type and *daf-16* mutant *Caenorhabditis elegans*. (A) Fluorescent microscopic observation of *C. elegans*. (B) Quantification of fluorescence intensity in *C. elegans*. The relative fluorescence intensities were measured by comparison with the CFS-treated group. Data are shown as mean ± standard deviations of three independent experiments. Significant differences compared with the control (*Escherichia coli* OP50-fed group, ***$p < 0.001$) and CFS-fed group (*E. coli* OP50 mixed with CFS, ###$p < 0.001$) are shown.
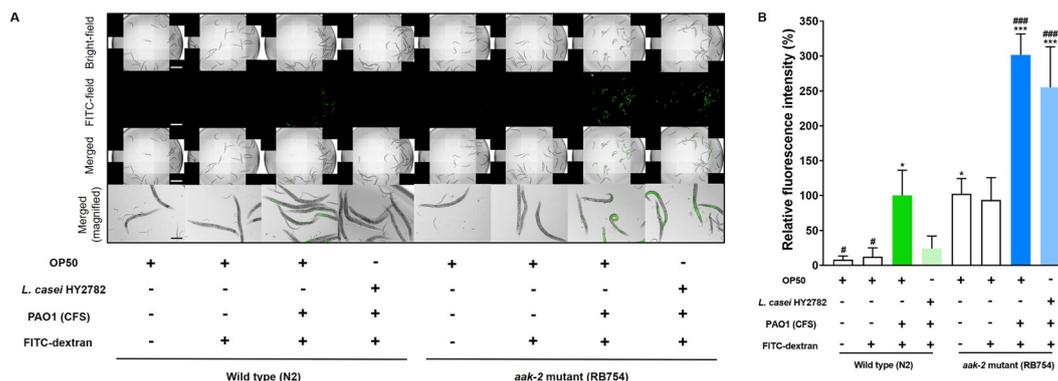
Fig. 6 Effect of *Lacticaseibacillus casei* HY2782 on *Pseudomonas aeruginosa* PAO1 cell-free supernatant (CFS)-induced intestinal permeability dysfunction in wild-type and *aak-2* mutant *Caenorhabditis elegans*. (A) Fluorescent microscopic observation of *C. elegans*. (B) Quantification of fluorescence intensity in *C. elegans*. The relative fluorescence intensities were measured by comparison with the CFS-treated group. Data are shown as means $\pm$ standard deviations of three independent experiments. Mean values were analyzed using one-way analysis of variance (ANOVA), followed by Tukey's range test. Significant differences compared with the control (*Escherichia coli* OP50-fed group, $*p < 0.05$ and $***p < 0.001$) and CFS-fed group (*E. coli* OP50 mixed with CFS, $\#p < 0.05$ and $\#\#\#p < 0.001$) are shown.

Table 1 Effect of Lacticaseibacillus casei HY2782 consumption on the lifespan of *Caenorhabditis elegans* treated with *Pseudomonas aeruginosa* cell-free supernatant (CFS)

Food source	Lifespan (days)			*p*-Values
	Minimum	Maximum	Mean	
Escherichia coli OP50	4	21	8.5 ± 0.3	<0.001
Lacticaseibacillus casei HY2782	4	25	12.1 ± 0.4	

Data are shown as mean ± standard deviation of each group. Significant difference was determined using the log-rank test.

(Day 10 of adulthood). The Smurf phenotype appeared in 34.8% (8/24 worms) of *E. coli* OP50-fed aged worms, which exhibited aging-induced intestinal permeability. In contrast, only three Smurf worms (total of 23 worms) were found in the *L. casei* HY2782-fed aged worms ($p < 0.001$) (Fig. 8).

3.5 *L. casei* HY2782 induced *gst-4* expression in *C. elegans*

To assess whether *gst-4* gene expression contributed to intestinal damage prevention in *C. elegans*, GFP fluorescence intensity was measured in CL2166 worms, which contained the *gst-4p::GFP* reporter construct. Upon exposure to *L. casei* HY2782 (without *P. aeruginosa* CFS), the CL2166 worms exhibited a significant increase in fluorescence intensity from 100.0% to 127.9% ($p < 0.05$), 161.8% ($p < 0.01$), and 168.1% ($p < 0.05$) at 24, 48, and 72 h, respectively. Worms exposed to the *P. aeruginosa* CFS showed increased green fluorescence intensity (140.4%) at 24 h. However, the worms did not maintain GFP expression at 48 h (92.0%) or 72 h (107.5%) ($p > 0.05$), whereas GFP expression in worms exposed to CFS and *L. casei*
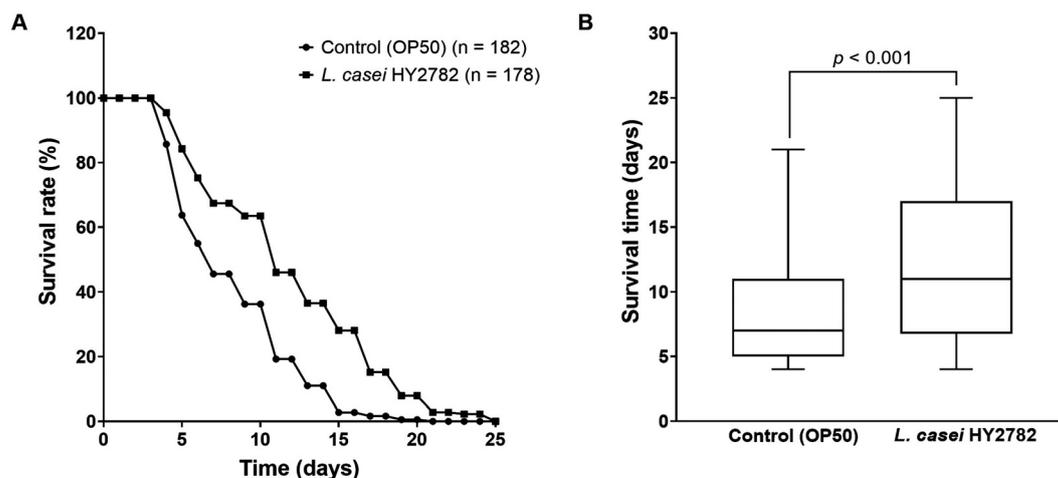

Fig. 7 Effect of *Lacticaseibacillus casei* HY2782 on the lifespan of *Caenorhabditis elegans* treated with the cell-free supernatant of *Pseudomonas aeruginosa* PAO1. (A) Lifespan curve. (B) Box plot analysis of *C. elegans*. The two groups were compared using the log-rank test. A total of 182 and 178 worms were used as the control and *L. casei* HY2782-fed groups, respectively.
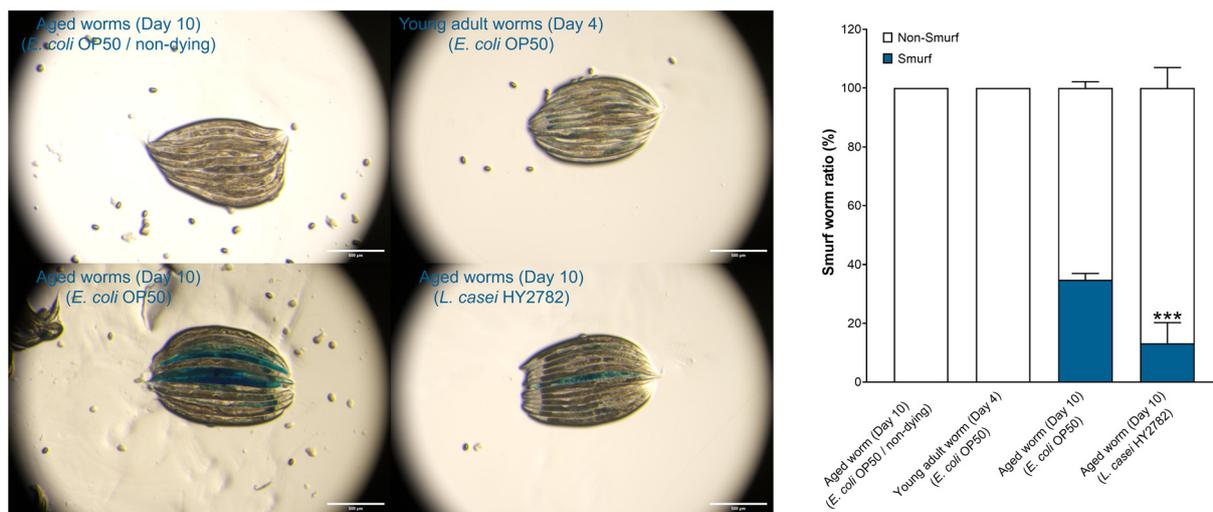
Fig. 8 Detection of age-related intestinal permeability dysfunction in *Caenorhabditis elegans*. The diffusion of blue dye is clearly visible throughout the body in Smurf worms with age-induced intestinal permeability. Observations were performed at a magnification of 7× (scale bar = 500 μm). The worm groups (*Escherichia coli* OP50-fed or *Lacticaseibacillus casei*-fed group) were compared using a binomial test at $p < 0.05$. Data are shown as means ± standard deviations of two independent experiments.

HY2782 increased to 238.6%, 222.6% ($p < 0.001$), and 227.7% ($p < 0.001$) at 24, 48, and 72 h, respectively. In addition, significant differences were observed between worms exposed to CFS alone and those exposed to *L. casei* HY2782 and CFS at 24, 48, and 72 h ($p < 0.001$) (Fig. 9). These data imply that *L. casei* HY2782 consumption increased *gst-4* expression, which plays an important role in the removal of oxidative stress during *P. aeruginosa* infection.[29]

3.6 SCFA production under simulated colonic fecal fermentation with *L. casei* HY2782

SCFAs are metabolized end-products of fermentation by the gut microbiota and are closely associated with human health benefits.[30–33] SCFA production in the GI tract is affected by the microbiome niche; therefore, the SCFA concentration was measured under simulated colonic fecal fermentation conditions. In normal colon condition, the vehicle group increased acetate concentration (up to 88.2 mM) and propionate and butyrate was rarely measured during fermentation (Fig. 10A). However, *L. casei* HY2782 consistently increased butyrate concentration (from 21.0 mM to 93.4 mM) and inhibited acetate production during fermentation in normal colon condition (Fig. 10B). In vehicle group of high-protein diet colon condition, acetate was the most abundant SCFA whereas that of propionate and butyrate production was inhibited during fermentation (Fig. 10C). Compared with those in the vehicle group, the *L. casei* HY2782 increased butyrate concentration from 78.0 mM to 114,78 mM whereas acetate and pro-
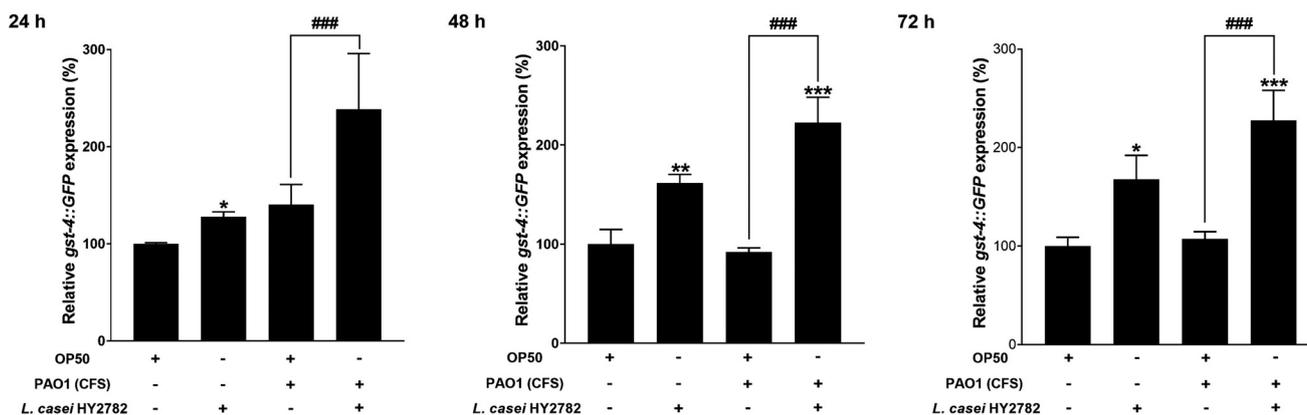

Fig. 9 The *gst-4p::GFP* expression in *Caenorhabditis elegans* CL2166. Mean values were analyzed using one-way analysis of variance (ANOVA), followed by Games-Howell test (24 h) and Tukey's range test (48 h and 72 h). Significant differences compared with the vehicle control (*Escherichia coli* OP50-fed group without the cell-free supernatant of *Pseudomonas aeruginosa* PAO1 (CFS), *$p < 0.05$, **$p < 0.01$, and ***$p < 0.001$). Significant differences between the CFS-fed group (*E. coli* OP50 with CFS) and the *Lacticaseibacillus casei* HY2782-fed group (*L. casei* HY2782 with CFS, ###$p < 0.001$) are shown.
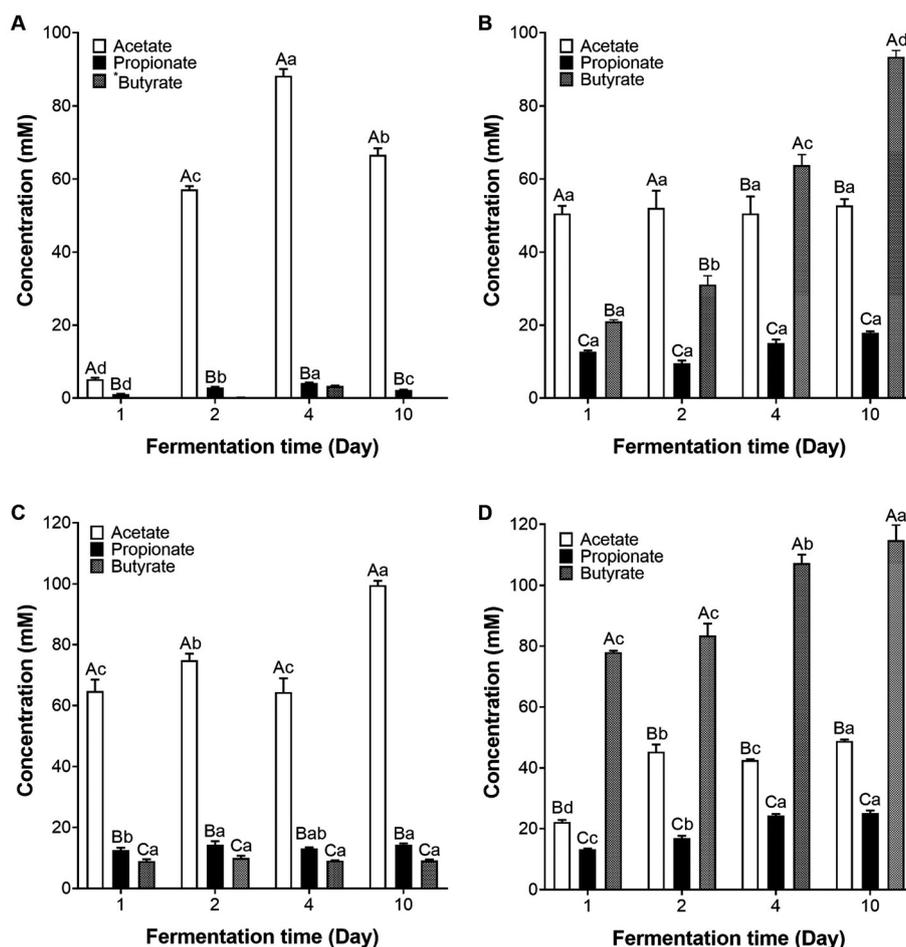
Fig. 10 Short-chain fatty acid (SCFA) production under artificial colonic fecal fermentation. (A) Changes in SCFA content under normal colon conditions (vehicle control). (B) Changes in SCFA content under normal colon conditions fermented with *L. casei* HY2782. (C) Changes in SCFA content under high-protein diet conditions (vehicle control). (D) Changes in SCFA content under high-protein diet conditions fermented with *L. casei* HY2782. Mean values were analyzed using one-way analysis of variance (ANOVA), followed by Duncan's multiple range test. Different uppercase letters indicate significant differences of SCFA type within the equal fermentation time. Different lower case letters indicate significant differences of SCFA concentration during fermentation (acetate, propionate, and butyrate, respectively).

pionate slightly increased from 22.2 mM to 48.9 mM and 13.2 mM to 25.2 mM, respectively (Fig. 10D).

3.7 Microbiome diversity under simulated colonic fecal fermentation

Microbial diversity in the simulated colon was measured to analyze changes in the microbiome niche of the GI tract. After fermentation, the OTU levels differed between the control and *L. casei* HY2782-fortified groups. At the phylum level, Firmicutes (containing order Lactobacillales) increased, whereas Bacteroidetes decreased in the *L. casei* HY2782-fermented group (Fig. 11A). Considering alpha diversity (Shannon index), *L. casei* HY2782 showed the potential to proliferate in the GI tract and inhibit other opportunistic pathogens, such as Bacteroidetes (Fig. 11B). During fermentation, *L. casei* HY2782 assisted in the growth of *Faecalibacterium* and *Lachnospira*, which belong to a butyrate-producing family ($p <$

0.01), whereas *Fusobacterium* growth was inhibited ($p < 0.05$) (Fig. 11D and E).

3.8 Lifespan of fermented product-fed *C. elegans*

Finally, *C. elegans* worms were fed fermented product samples. The survival curves are presented in Fig. 12 and the mean lifespans are summarized in Table 2. Briefly, worms fed with normal colonic ferments had a mean lifespan of 10.3 ± 0.2 days. Feeding with *L. casei* HY2782-incoulated fecal ferments from the normal colon increased the mean lifespan to 14.5 ± 0.3 days ($p < 0.001$, Table 2). Feeding with high-protein diet colon ferments shortened the mean lifespan to 7.9 ± 0.1 days, whereas feeding with the high-protein diet colon ferments containing *L. casei* HY2782 resulted in the mean lifespan of 13.7 ± 0.2 ($p < 0.001$). Altogether, the lifespan of *C. elegans* significantly increased when fed *L. casei* HY2782-fermented product.
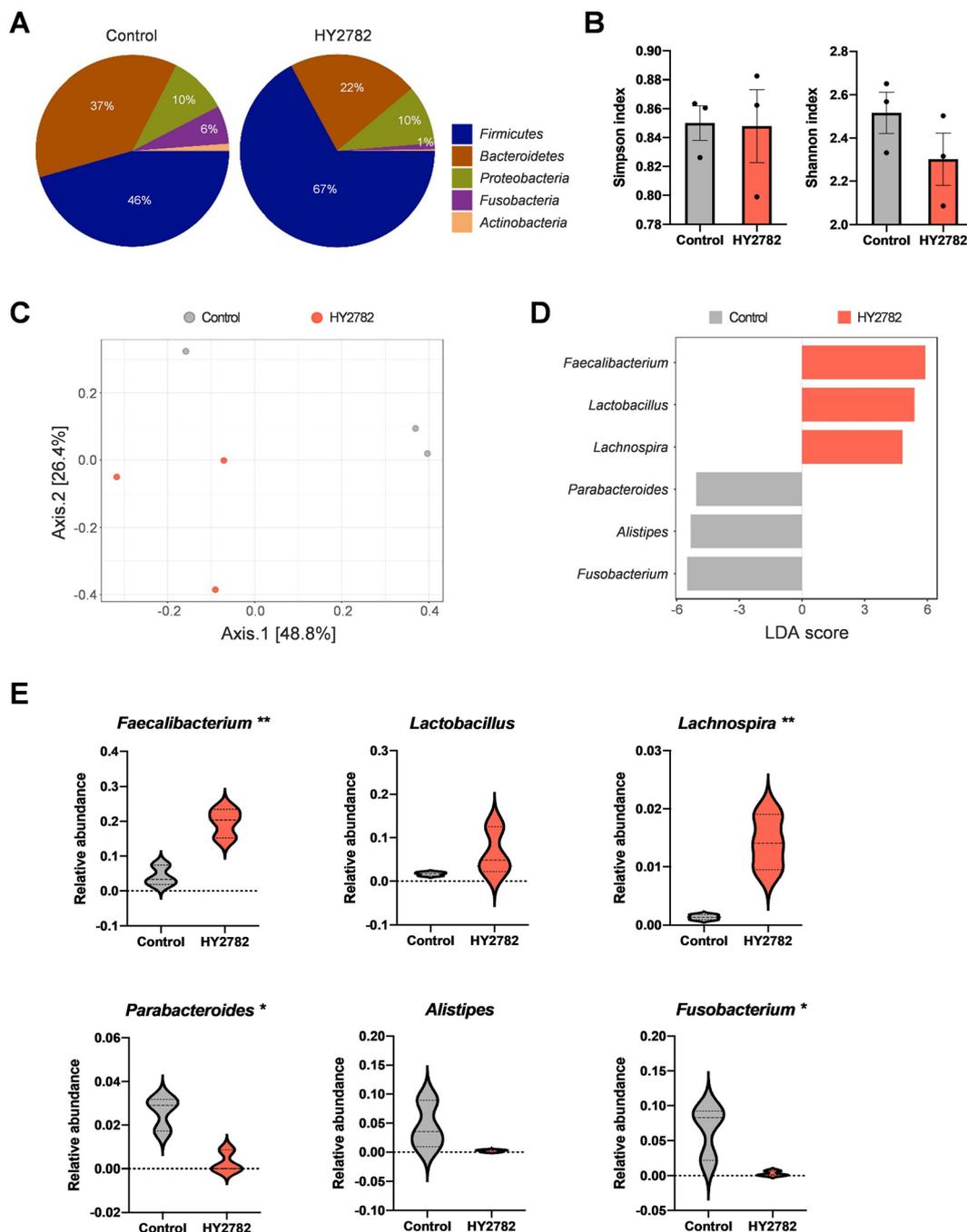
Fig. 11 Effect of *Lacticaseibacillus casei* HY2782 on microbial composition under artificial colonic fecal fermentation conditions. (A) The phylum-level microbial composition of the vehicle control and *L. casei* HY2782-inoculated groups. (B) The α-diversity analysis of fermented samples. Simpson and Shannon index values for microbial evenness were calculated to investigate the α-diversity of each group. Data are shown as the mean ± standard deviations. (C) Principal coordinate analysis (PCoA) score plot. Bray–Curtis dissimilarity was used to generate the ordination of β-diversity between two groups. (D) Histograms of the linear discriminant analysis scores for differentially abundant microbiota (genus level) between two groups. (E) Violin plots showing the relative abundances for six discriminative genera. Significance was assessed using the student's *t*-test (*p < 0.05 and **p < 0.01).

4.   Discussion

The intestinal microbiome plays a critical role in protein metabolism.[34] The proteolytic activity of the intestinal micro-biome contributes to the development of a metabolite pool

and regulates amino acids in the intestine.[31] Acetate and pro-pionate mainly accumulate in the intestine during dietary protein fermentation in the GI tract,[35] whereas butyrate accumulates *via* a restricted pathway—the acetate-CoA-transfer-ase pathway—in Firmicutes.[36] In addition, butyrate is syn-
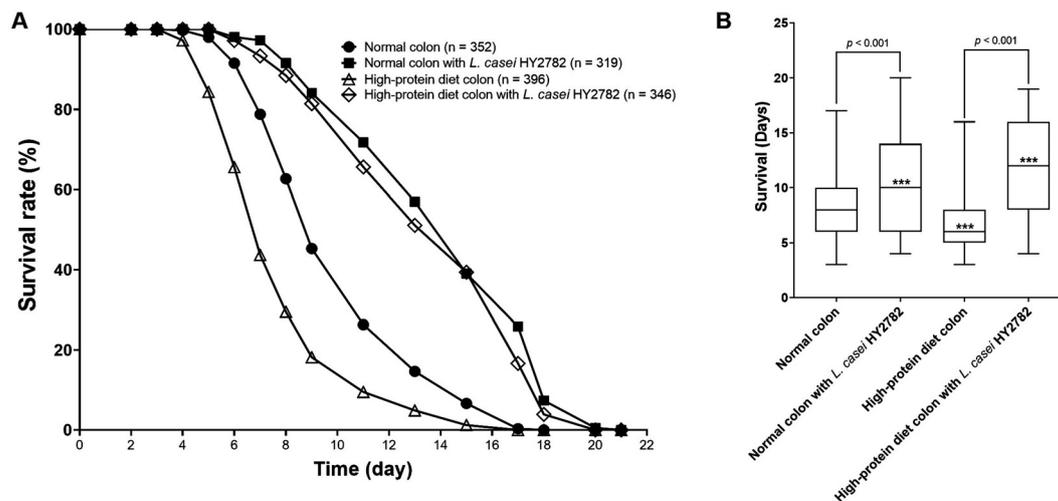
Fig. 12 Lifespan of *Caenorhabditis elegans* fed *Lacticaseibacillus casei* HY2782– fermented product from artificial colonic fecal fermentation. (A) Lifespan curve of *C. elegans*. (B) Median and maximum lifespan of *C. elegans*. The two groups were compared using the log-rank test. Significant differences compared with the normal vehicle control group (***$p < 0.001$) are shown.

Table 2 Lifespan of *Caenorhabditis elegans* fed fecal fermentation products

Artificial colonic conditions		Lifespan (days)			*p*-Values
		Minimum	Maximum	Mean	
Normal	Control	3	17	10.3 ± 0.2	<0.001
	Lacticaseibacillus casei HY2782	4	20	14.5 ± 0.3	
High-protein diet	Control	3	16	7.9 ± 0.1	<0.001
	Lacticaseibacillus casei HY2782	4	19	13.7 ± 0.2	

Data are shown as mean ± standard deviation of each group. Significant difference was determined using the log-rank test.

thesized from amino acids, such as lysine and glutamine,[37] and organic acids, such as succinate and lactate.[32] Furthermore, butyrate contributes to healthy GI tract conditions by regulating the microbial niche and inflammation, reinforcing the mucosal barrier, and promoting epithelial growth.[38] In a high-protein diet, proteolytic fermentation decreases butyrate levels and induces inflammatory reactions and cardiovascular diseases.[39] Therefore, several studies have investigated butyrate production by LAB to improve GI tract conditions. For example, Moens *et al.*[32] investigated four LAB species (*Lactobacillus acidophilus*, *Lactiplantibacillus plantarum*, *Lacticaseibacillus rhamnosus*, and *Enterococcus faecium*) that promote the production of butyrate and IL-10, an anti-inflammatory cytokine produced in human intestinal models. In a clinical trial, Ford *et al.*[39] reported that a high-protein diet suppressed butyrate production, and probiotic supplements containing *Bifidobacterium longum*, *Bifidobacterium breve*, *L. acidophilus*, and *L. plantarum* relieved indigestion in high-protein diet consumers. In this study, *L. casei* HY2782 supplementation increased butyrate production during the simulated colon fermentation, which aligns well with previous studies.

The human body comprises the following bacterial phyla: Firmicutes, Bacteroidetes, Proteobacteria, Fusobacteria, Actinobacteria, and Verrucomicrobia.[33] These bacteria interact with the host by secreting metabolites, such as SCFAs, ρ-cresol, ρ-cresyl-glucuronide, indole-3 acetic acid, indoxyl sulfate, and trimethylamine *N*-oxide.[40] The Firmicutes/Bacteroidetes (F/B) ratio is a necessary index for maintaining homeostasis.[33] Stojanov *et al.*[33] reported that an imbalance when the F/B ratio is decreased causes inflammatory bowel disease. Moreover, an imbalance in the F/B ratio has also been observed in an intestinal bowel disease mouse model.[41] *Faecalibacterium*[36,37] and *Lachnospira*[32,37] are representative genera of butyrate producers, which are members of the Firmicutes. Notably, *L. casei* HY2782 enhanced the *Faecalibacterium* and *Lachnospira* ratio during the simulated colonic fecal fermentation, which increased the F/B ratio, thereby resulting in butyrate production.

Nematodes and humans share conserved aging mechanisms. For example, DAF-16 and SKN-1, orthologs of human forkhead box protein O (FOXO) and nuclear factor erythroid 2-related factor 2 (Nrf2), respectively, play critical roles in regulating aging, stress responses, metabolism, and homeostasis in *C. elegans*.[11] Lee and Lee[12] reported that insulin/insulin-like growth factor-1 (IGF-1) signaling (IIS), regulated by the DAF-2/IGF-1 receptor (IGFR), affects aging in diverse species, ranging

from *C. elegans* to mammals. The IIS cascade inhibits the phosphorylation of DAF-2/IGFR, thus resulting in its cytoplasmic retention.[11,12] The anti-aging effects of IIS inhibition and translocation of DAF-16/FOXO and SKN-1/Nrf2 have been investigated.[11] Adenosine monophosphate-activated protein kinase-2 (AAK-2/AMPK), encoded by *aak-2* in *C. elegans*, is also crucial in aging.[42] AAK-2/AMPK mediates the phosphorylation of DAF-16/FOXO[42,43] and the DAF-16/FOXO-dependent transcription of superoxide dismutase to extend the lifespan of *C. elegans*.[43] Onken and Driscoll[44] suggested that AAK-2/AMPK activates SKN-1/Nrf2 translocation to regulate reactive oxygen species. Additionally, Peng *et al.*[45] showed that the AAK-2/AMPK pathway is involved in the antioxidant mechanism of chicoric acid in *aak-2* mutant worm strains. Similarly, this study suggests that AAK-2/AMPK, DAF-16/FOXO, and SKN-1/Nrf2 play essential roles in the *L. casei* HY2782-induced longevity of *C. elegans*, as evidenced by the experiments in which *L. casei* HY2782 was consumed by *aak-2*, *daf-16*, and *skn-1* mutant worms, respectively.

Glutathione (GSH) is another critical factor affecting the lifespan of *C. elegans*.[11,46] Similar to IIS, GSH biosynthesis in *C. elegans* resembles that of mammals. In *C. elegans*, the SKN-1/Nrf-2 transcription factor promotes gamma-glutamylcysteine synthetase and GST-4, which are phase II detoxification enzymes that resist oxidative or xenobiotic stress.[13] Ferguson and Bridge[46] suggested that *C. elegans* has 56 GST genes that encode specific GSTs in response to certain xenobiotic compounds. Thus, *gst-4* expression in *C. elegans* damaged by *P. aeruginosa* is related to a specific reaction, and *L. casei* HY2782 probably promotes *gst-4* expression to attenuate this damage.

5. Conclusions

This study demonstrates improvements in intestinal permeability and lifespan extension in *C. elegans* as a result of consumption of the probiotic bacteria *L. casei* HY2782. Moreover, this study is the first to mimic the intestinal system by combining aerobic fecal fermentation and the model nematode *C. elegans*. *L. casei* HY2782 consumption prevented intestinal permeability dysfunction and prolonged the lifespan of *C. elegans* through the DAF-16/FOXO and SKN-1/NRF2 molecular pathways. Furthermore, *gst-4* expression was upregulated by *L. casei* HY2782. Additionally, fermented media from the simulated colon fecal fermentation, which reconstructed the microbiome niche from human fecal samples, further supported lifespan extension in *C. elegans*. Overall, these findings suggest that *L. casei* HY2782 is a promising probiotic candidate for improving intestinal health as well as longevity.

Conflicts of interest

The authors declare no competing interests.

Data availability

Acknowledgements

References

1 M. Snelson, R. E. Clarke, T. V. Nguyen, S. A. Penfold, J. M. Forbes, S. M. Tan and M. T. Coughlan, Long term high protein diet feeding alters the microbiome and increases intestinal permeability, systemic inflammation and kidney injury in mice, *Mol. Nutr. Food Res.*, 2021, **65**, e2000851.

2 J. Roberts, A. Zinchenko, K. T. Mahbubani, J. Johnstone, L. Smith, V. Merzbach, M. Blacutt, O. Banderas, L. Villasenor, F. T. Vårvik and M. Hanselmans, Satiating effect of high protein diets on resistance-trained in energy deficit, *Nutrients*, 2018, **11**, 56.

3 M. J. Skytte, A. Samkani, A. D. Petersen, M. N. Thomsen, A. Astrup, E. Chabanova, J. Frystyk, J. J. Holst, H. S. Thomsen, S. Madsbad, T. M. Larsen, S. B. Haugaard and T. Krarup, A carbohydrate-reduced high-protein diet improves HbA_{1c} and liver fat content in weight stable participants with type 2 diabetes: A randomised controlled trial, *Diabetologia*, 2019, **62**, 2066–2078.

4 A. Kumar, T. Joishy, S. Das, M. C. Kalita, A. K. Mukherjee and M. R. Khan, A potential probiotic Lactobacillus plantarum JBC5 improves longevity and healthy aging by modulating antioxidative, innate immunity and serotonin-signaling pathways in *Caenorhabditis elegans*, *Antioxidants*, 2022, **11**, 268.

5 M. Roselli, E. Schifano, B. Guantario, P. Zinno, D. Uccelletti and C. Devirgiliis, *Caenorhabditis elegans* and probiotics interactions from a prolongevity perspective, *Int. J. Mol. Sci.*, 2019, **20**, 5020.

6 S. Kishimoto, M. Nono, Y. Makizaki, Y. Tanaka, H. Ohno, E. Nishida and M. Uno, *Lactobacillus paracasei* subsp. *para-*

casei, 2004 improves health and lifespan in *Caenorhabditis elegans*, *Sci. Rep.*, 2024, **14**, 10453.

7 U. T. T. Nguyen, E. Youn, T. A. N. Le, N. M. Ha, S. H. Tran, S. Lee, J. W. Cha, J. S. Park, H. C. Kwon and K. Kang, Photodynamic treatment increases the lifespan and oxidative stress resistance of *Caenorhabditis elegans*, *Free Radicals Biol. Med.*, 2024, **221**, 98–110.

8 N. M. Ha, S. H. Tran, Y. H. Shim and K. Kang, *Caenorhabditis elegans* as a powerful tool in natural product bioactivity research, *Appl. Biol. Chem.*, 2022, **65**, 18.

9 A. N. Kang, D. Mun, S. Ryu, J. J. Lee, S. Oh, M. K. Kim, M. Song, S. Oh and Y. Kim, Culturomic-, metagenomic-, and transcriptomic-based characterization of commensal lactic acid bacteria isolated from domestic dogs using *Caenorhabditis elegans* as a model for aging, *J. Anim. Sci.*, 2022, **100**, 1–16.

10 T. A. N. Le, B. Selvaraj, J. W. Lee and K. Kang, Measuring the effects of bacteria and chemicals on the intestinal permeability of *Caenorhabditis elegans*, *J. Visualized Exp.*, 2019, **154**, e60419.

11 R. Li, Q. Yi, J. Wang, Y. Miao, Q. Chen, Y. Xu and M. Tao, Paeonol promotes longevity and fitness in *Caenorhabditis elegans* through activating the DAF-16/FOXO and SKN-1/Nrf2 transcription factors, *Biomed. Pharmacother.*, 2024, **173**, 116368.

12 H. Lee and S. V. Lee, Recent progress in regulation of aging by insulin/IGF-1 signaling in *Caenorhabditis elegans*, *Mol. Cells*, 2022, **45**, 763–770.

13 A. Zhu, F. Zheng, W. Zhang, L. Li, Y. Li, Y. Hu, Y. Wu, W. Bao, G. Li, Q. Wang and H. Li, Oxidation and antioxidation of natural products in the model organism *Caenorhabditis elegans*, *Antioxidants*, 2022, **11**, 705.

14 C. T. S. Ana, J. Ju, F. A. R. de Barros and K. H. Kim, Macauba (*Acrocomia aculeata*) pulp oil reduces fat accumulation and enhances the lifespan of *Caenorhabditis elegans* at low temperatures via *fat*-1- and *fat*-7-dependent pathway, *J. Food Sci.*, 2024, **89**, 5101–5112.

15 Y. Cui and X. Qu, Genetic mechanisms of prebiotic carbohydrate metabolism in lactic acid bacteria: Emphasis on *Lacticaseibacillus casei* and *Lacticaseibacillus paracasei* as flexible, diverse and outstanding prebiotic carbohydrate starters, *Trends Food Sci. Technol.*, 2021, **115**, 486–499.

16 D. W. Olson and K. J. Aryana, Probiotic incorporation into yogurt and various novel yogurt-based products, *Appl. Sci.*, 2022, **12**, 12607.

17 X. Ma, Y. J. Shin, H. S. Park, J. W. Jeong, J. Y. Kim, J. J. Shim, J. L. Lee and D. H. Kim, *Lactobacillus casei* and its supplement alleviate stress-induced depression and anxiety in mice by the regulation of BDNF expression and NF-κB activation, *Nutrients*, 2023, **15**, 2488.

18 J. Y. Kim, S. Y. Lee, S. H. Jung, M. R. Kim, I. D. Choi, J. L. Lee, J. H. Sim, C. H. Pan and K. Kang, Protective effect of *Lactobacillus casei* HY2782 against particulate matter toxicity in human intestinal CCD-18Co cells and *Caenorhabditis elegans*, *Biotechnol. Lett.*, 2020, **42**, 519–528.

19 J. Y. Kim, T. A. N. Le, S. Y. Lee, D. G. Song, S. C. Hong, K. H. Cha, J. W. Lee, C. H. Pan and K. Kang, 3,3′-

20 Diindolylmethane improves intestinal permeability dysfunction in cultured human intestinal cells and the model animal *Caenorhabditis elegans*, *J. Agric. Food Chem.*, 2019, **67**, 9277–9285.

20 M. R. Kim, S. Y. Cho, H. H. Lee, J. Y. Kim, U. T. T. Nguyen, N. M. Ha, K. Y. Choi, K. H. Cha, J. H. Kim, W. K. Kim and K. Kang, Schisandrin C improves leaky gut conditions in intestinal cell monolayer, organoid, and nematode models by increasing tight junction protein expression, *Phytomedicine*, 2022, **103**, 154209.

21 A. C. Walker, R. Bhargava, M. J. Bucher, Y. M. Argote, A. S. Brust and D. M. Czyż, Identification of proteotoxic and proteoprotective bacteria that non-specifically affect proteins associated with neurodegenerative diseases, *iScience*, 2024, **27**, 110828.

22 S. Gelino, J. T. Chang, C. Kumsta, X. She, A. Davis, C. Nguyen, S. Panowski and M. Hansen, Intestinal autophagy improves healthspan and longevity in *C. elegans* during dietary restriction, *PLoS Genet.*, 2016, **12**, e1006135.

23 J. B. Jin, J. W. Cha, I. S. Shin, J. Y. Jeon, K. H. Cha and C. H. Pan, Supplementation with *Chlorella vulgaris*, *Chlorella protothecoides*, and *Schizochytrium* sp. increases propionate-producing bacteria in *in vitro* human gut fermentation, *J. Sci. Food Agric.*, 2020, **100**, 2938–2945.

24 K. H. Cha, E. H. Lee, H. S. Yoon, J. H. Lee, J. Y. Kim, K. Kang, J. S. Park, J. B. Jin, G. Ko and C. H. Pan, Effects of fermented milk treatment on microbial population and metabolomic outcomes in a three-stage semi-continuous culture system, *Food Chem.*, 2018, **263**, 216–224.

25 S. Scortichini, M. C. Boarelli, S. Silvi and D. Fiorini, Development and validation of a GC-FID method for the analysis of short chain fatty acids in rat and human faeces and in fermentation fluids, *J. Chromatogr. B:Anal. Technol. Biomed. Life Sci.*, 2020, **1143**, 121972.

26 D. W. Fadrosh, B. Ma, P. Gajer, N. Sengamalay, S. Ott, R. M. Brotman and J. Ravel, An improved dual-indexing approach for multiplexed 16S rRNA gene sequencing on the Illumina MiSeq platform, *Microbiome*, 2014, **2**, 6.

27 E. Bolyen, J. R. Rideout, M. R. Dillon, N. A. Bokulich, C. C. Abnet, G. A. Al-Ghalith, H. Alexander, E. J. Alm, M. Arumugam, F. Asnicar, Y. Bai, J. E. Bisanz, K. Bittinger, A. Brejnrod, C. J. Brislawn, C. T. Brown, B. J. Callahan, A. M. Caraballo-Rodríguez, J. Chase, E. K. Cope, R. Da Silva, C. Diener, P. C. Dorrestein, G. M. Douglas, D. M. Durall, C. Duvallet, C. F. Edwardson, M. Ernst, M. Estaki, J. Fouquier, J. M. Gauglitz, S. M. Gibbons, D. L. Gibson, A. Gonzalez, K. Gorlick, J. Guo, B. Hillmann, S. Holmes, H. Holste, C. Huttenhower, G. A. Huttley, S. Janssen, A. K. Jarmusch, L. Jiang, B. D. Kaehler, K. B. Kang, C. R. Keefe, P. Keim, S. T. Kelley, D. Knights, I. Koester, T. Kosciolek, J. Kreps, M. G. I. Langille, J. Lee, R. Ley, Y. X. Liu, E. Loftfield, C. Lozupone, M. Maher, C. Marotz, B. D. Martin, D. McDonald, L. J. McIver, A. V. Melnik, J. L. Metcalf, S. C. Morgan, J. T. Morton, A. T. Naimey, J. A. Navas-Molina, L. F. Nothias, S. B. Orchanian, T. Pearson, S. L. Peoples, D. Petras,

M. L. Preuss, E. Pruesse, L. B. Rasmussen, A. Rivers, M. S. Robeson, P. Rosenthal, N. Segata, M. Shaffer, A. Shiffer, R. Sinha, S. J. Song, J. R. Spear, A. D. Swafford, L. R. Thompson, P. J. Torres, P. Trinh, A. Tripathi, P. J. Turnbaugh, S. Ul-Hasan, J. J. J. van der Hooft, F. Vargas, Y. Vázquez-Baeza, E. Vogtmann, M. von Hippel, W. Walters, Y. Wan, M. Wang, J. Warren, K. C. Weber, C. H. D. Williamson, A. D. Willis, Z. Z. Xu, J. R. Zaneveld, Y. Zhang, Q. Zhu, R. Knight and J. G. Caporaso, Reproducible, interactive, scalable and extensible microbiome data science using QIIME 2, *Nat. Biotechnol.*, 2019, **37**, 852–857.

28 Y. Lu, G. Zhou, J. Ewald, Z. Pang, T. Shiri and J. Xia, MicrobiomeAnalyst 2.0: Comprehensive statistical, functional and integrative analysis of microbiome data, *Nucleic Acids Res.*, 2023, **51**, W310–W318.

29 R. van der Hoeven, K. C. McCallum, M. R. Cruz and D. A. Garsin, Ce-Duox1/BLI-3 generated reactive oxygen species trigger protective SKN-1 activity via p38 MAPK signaling during infection in *C. elegans*, *PLoS Pathog.*, 2011, **7**, e1002453.

30 A. Oliver, Z. Alkan, C. B. Stephensen, J. W. Newman, M. E. Kable and D. G. Lemay, Diet, microbiome, and inflammation predictors of fecal and plasma short-chain fatty acids in humans, *J. Nutr.*, 2024, **11**, 3298–3311.

31 R. Jäger, J. Zaragoza, M. Purpura, S. Iametti, M. Marengo, G. M. Tinsley, A. J. Anzalone, J. M. Oliver, W. Fiore, A. Biffi, S. Urbina and L. Taylor, Probiotic administration increases amino acid absorption from plant protein: A placebo-controlled, randomized, double-blind, multicenter, crossover study, *Probiotics Antimicrob. Proteins*, 2020, **12**, 1330–1339.

32 F. Moens, P. Van den Abbeele, A. W. Basit, C. Dodoo, R. Chatterjee, B. Smith and S. Gaisford, A four-strain probiotic exerts positive immunomodulatory effects by enhancing colonic butyrate production *in vitro*, *Int. J. Pharm.*, 2019, **555**, 1–10.

33 S. Stojanov, A. Berlec and B. Štrukelj, The influence of probiotics on the Firmicutes/Bacteroidetes ratio in the treatment of obesity and inflammatory bowel disease, *Microorganisms*, 2020, **8**, 1715.

34 F. Mei, Z. Duan, M. Chen, J. Lu, M. Zhao, L. Li, X. Shen, G. Xia and S. Chen, Effect of a high-collagen peptide diet on the gut microbiota and short-chain fatty acid metabolism, *J. Funct. Foods*, 2020, **75**, 104278.

35 P. Markowiak-Kopeć and K. Śliżewska, The effect of probiotics on the production of short-chain fatty acids by human intestinal microbiome, *Nutrients*, 2020, **12**, 1107.

36 S. Kim, S. Park, T. G. Choi and S. S. Kim, Role of short chain fatty acids in epilepsy and potential benefits of probiotics and prebiotics: Targeting "health" of epileptic patients, *Nutrients*, 2022, **14**, 2982.

37 S. Zhao, R. Lau, Y. Zhong and M. H. Chen, Lactate cross-feeding between *Bifidobacterium* species and *Megasphaera indica* contributes to butyrate formation in the human colonic environment, *Appl. Environ. Microbiol.*, 2024, **90**, e0101923.

38 J. Zhang, L. Zhong, S. Chi, W. Chu, Y. Liu and Y. Hu, Sodium butyrate supplementation in high-soybean meal diets for juvenile rice field eel (*Monopterus albus*): Effects on growth, immune response and intestinal health, *Aquaculture*, 2020, **520**, 734952.

39 A. L. Ford, V. Nagulesapillai, A. Piano, J. Auger, S. A. Girard, M. Christman, T. A. Tompkins and W. J. Dahl, Microbiota stability and gastrointestinal tolerance in response to a high-protein diet with and without a prebiotic, probiotic, and synbiotic: A randomized, double-blind, placebo-controlled trial in older women, *J. Acad. Nutr. Diet.*, 2020, **120**, 500–516.

40 H. Usuda, T. Okamoto and K. Wada, Leaky gut: Effect of dietary fiber and fats on microbiome and intestinal barrier, *Int. J. Mol. Sci.*, 2021, **22**, 7613.

41 F. Wan, H. Han, R. Zhong, M. Wang, S. Tang, S. Zhang, F. Hou, B. Yi and H. Zhang, Dihydroquercetin supplement alleviates colonic inflammation potentially through improved gut microbiota community in mice, *Food Funct.*, 2021, **12**, 11420–11434.

42 A. Mallick, A. Ranawade, W. van den Berg and B. P. Gupta, Axin-mediated regulation of lifespan and muscle health in *C. elegans* requires AMPK-FOXO signaling, *iScience*, 2020, **23**, 101843.

43 M. Hao, Z. Zhang, Y. Guo, H. Zhou, Q. Gu and J. Xu, Rubidium chloride increases life span through an AMPK/FOXO-dependent pathway in *Caenorhabditis elegans*, *J. Gerontol., Ser. A*, 2022, **77**, 1517–1524.

44 B. Onken and M. Driscoll, Metformin induces a dietary restriction–like state and the oxidative stress response to extend *C. elegans* healthspan via AMPK, LKB1, and SKN-1, *PLoS One*, 2010, **5**, e8758.

45 Y. Peng, Q. Sun, R. Gao and Y. Park, AAK-2 and SKN-1 are involved in chicoric-acid-induced lifespan extension in *Caenorhabditis elegans*, *J. Agric. Food Chem.*, 2019, **67**, 9178–9186.

46 G. D. Ferguson and W. J. Bridge, The glutathione system and the related thiol network in *Caenorhabditis elegans*, *Redox Biol.*, 2019, **24**, 101171.